ELSEVIER

# Effects of Co and Fe addition on the properties of lanthanum strontium manganite

S. Kuharuangrong[a,*], T. Dechakupt[b], P. Aungkavattana[c]

[a] School of Ceramic Engineering at Suranaree University of Technology, Nakhon Ratchasima 30000, Thailand
[b] Department of Materials Science, Chulalongkorn University, Bangkok 10330, Thailand
[c] National Metal and Materials Technology Center, Patumthani 12120, Thailand

## Abstract

The effects of Co and Fe dopants with the amount of 20 and 40 mol% on the properties of $La_{0.84}Sr_{0.16}MnO_3$ were investigated. All compositions were prepared by conventional mixed oxide process and sintered at 1450 °C. The structure of undoped and Co-doped compositions was found to be monoclinic. In addition, the second phase was observed in these sintered compositions. The conductivity of doped materials decreased as compared to that of $La_{0.84}Sr_{0.16}MnO_3$. The SEM microstructure showed the decrease of grain size as Co content increased. The thermal expansion coefficient (TEC) tended to increase as Co content increased. In contrast, the monoclinic and orthorhombic structures were found in 20 and 40 mol% Fe-doped $La_{0.84}Sr_{0.16}MnO_3$. The amount of second phase in sintered composition depends on the amount of Fe content. The conductivity at 1000 °C decreased, but the grain size increased as Fe content increased. The thermal expansion coefficient slightly changed with Fe addition.
© 2004 Elsevier B.V. All rights reserved.

## 1. Introduction

Lanthanum strontium manganite ($La_{1-x}Sr_xMnO_3$, LSM) is extensively used as cathode material for a solid oxide fuel cell (SOFC) because it offers high electronic conductivity, high catalytic activity for oxygen reduction and chemical and thermal compatibility with yttria-stabilized zirconia (YSZ) electrolyte at the operating temperature [1]. LSM is a perovskite oxide $ABO_3$ where $La^{3+}$ ions in the A-sites are partially substituted by $Sr^{2+}$ ions. Its structure has been reported to be rhombohedral [2–4] or monoclinic [5], depending on the amount of $Mn^{4+}$, which can be varied by sintering atmosphere, temperature and $Sr^{2+}$ content. $LaMnO_3$ is a p-type semiconductor due to small polaron hopping of holes [1]. Doping of Sr into $LaMnO_3$ increases the electrical conductivity considerably because a number of holes increase [1]. Nevertheless, an increase of Sr also increases the thermal expansion coefficient (TEC) [3,4]

and affects the chemical reaction with YSZ at high operating temperature [6–8], resulting in the degradation of cell performance.

To promote SOFC towards commercialization, there have been many attempts to develop the suitable materials for lower operating temperature below 900 °C without impeding its performance. The possible perovskite materials such as $LaCoO_3$ and $LaFeO_3$ have been studied. $LaCoO_3$ has much higher electrical conductivity than $LaMnO_3$, however, its thermal expansion coefficient is much greater than that of YSZ electrolyte [1]. In addition, it easily reacts with YSZ and forms the insulating layer at high temperature [1]. $LaFeO_3$ has higher catalytic activity for oxygen reduction at the lower temperature [9,10], possibly offering the good electrical properties. The objective of this work was to study the effect of Co or Fe addition into Lanthanum strontium manganite system. Although the other cations such as Mg, Ti and Nb [11] have been studied, Co and Fe are possible dopants to improve the properties of this composition. In this paper, $La_{0.84}Sr_{0.16}MnO_3$ was selected as the base material. The crystal structure, phase, thermal expansion coefficient and

* Corresponding author.
E-mail address: sutin@ccs.sut.ac.th (S. Kuharuangrong).
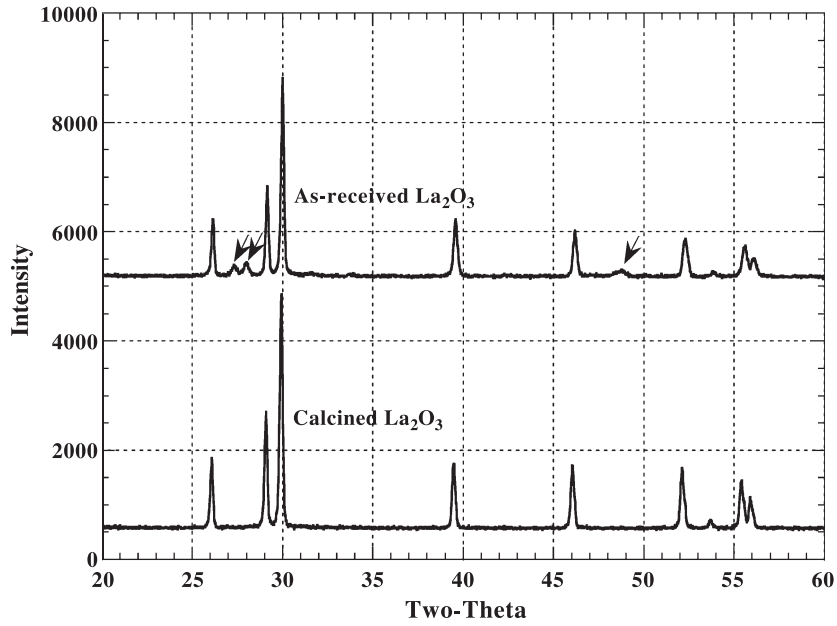
Fig. 1. XRD patterns of as-received $La_2O_3$ and calcined $La_2O_3$.

the electrical property of the modified composition were investigated.

## 2. Experimental

### 2.1. Sample preparation

Five compositions of $La_{0.84}Sr_{0.16}Mn_{1-x}B_xO_3$ (B = Co or Fe, $x = 0$, 0.2, 0.4) were prepared by conventional oxide

mixing process. The abbreviation of each composition is illustrated as follows:

$La_{0.84}Sr_{0.16}MnO_3$ (LSM)
$La_{0.84}Sr_{0.16}Mn_{0.8}Co_{0.2}O_3$ (LSMC2)
$La_{0.84}Sr_{0.16}Mn_{0.6}Co_{0.4}O_3$ (LSMC4)
$La_{0.84}Sr_{0.16}Mn_{0.8}Fe_{0.2}O_3$ (LSMF2)
$La_{0.84}Sr_{0.16}Mn_{0.6}Fe_{0.4}O_3$ (LSMF4)

Before batch preparation, the existing phases of each raw material were investigated by XRD (Jeol, JDX 3530), using
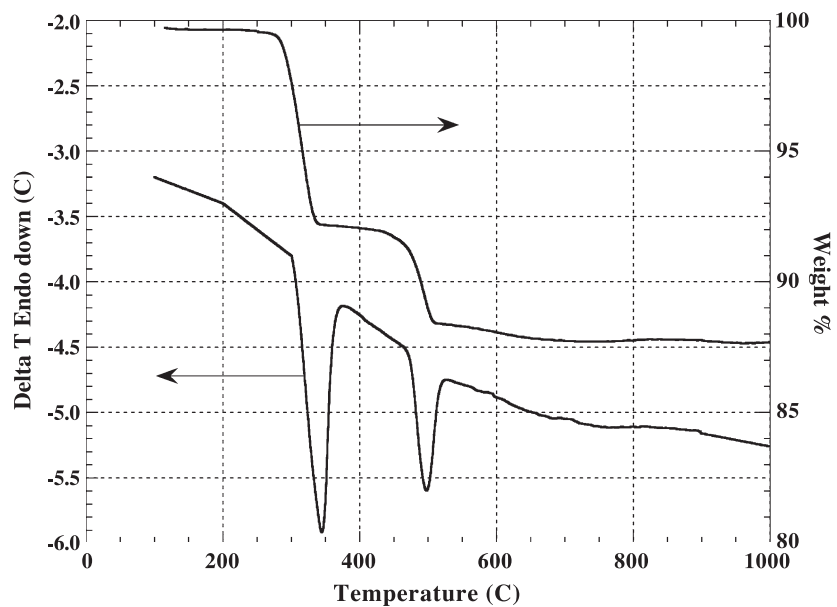


Fig. 2. DTA and TGA traces of as-received $La_2O_3$.
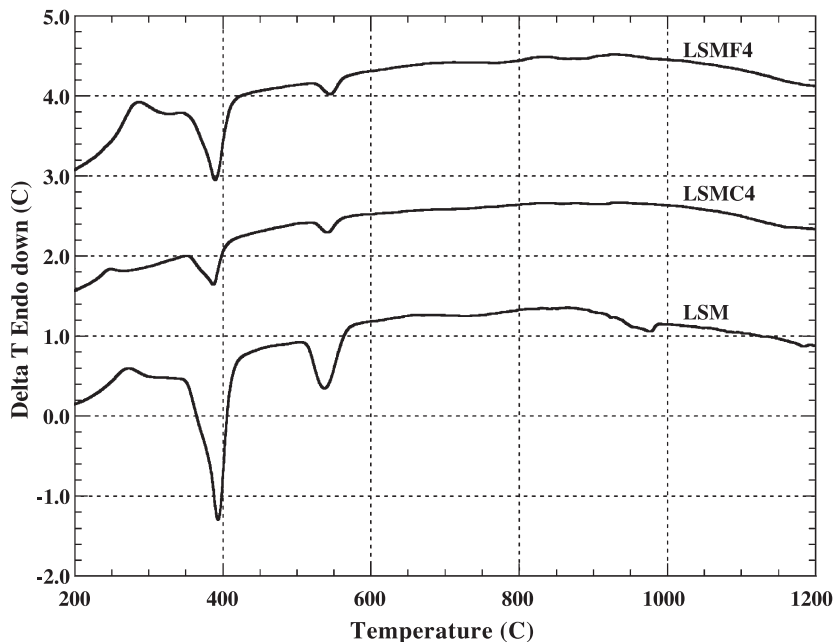
Fig. 3. DTA traces of mixed raw materials for LSM, LSMC4 and LSMF4.

CuK$_\alpha$ radiation and the undesirable phases, if existing, were eliminated by calcining to the temperatures obtained from the results of differential thermal analysis (DTA7, Perkin Elmer) and thermogravimetric analysis (TGA7, Perkin Elmer). The stoichiometric compositions were prepared by wet mixing in a polypropylene bottle, using alumina balls and absolute ethanol. After drying, the mixture was calcined with a heating rate of 3 °C/min. The appropriate calcining temperature of each composition was determined from the

result of DTA. After calcining, the phases and structures of all compositions were determined from XRD. Silicon was used as an internal standard for a correction of peak shifts.

The calcined powder was milled and dried before mixed with polyvinyl alcohol acted as binder and then formed into the rectangular bars by dry pressing. After binder burnout, the specimens were put on the alumina substrate covered with their calcined powder and sintered with a heating rate of 4 °C/min to 1450 °C with a soaking period for 2 h.
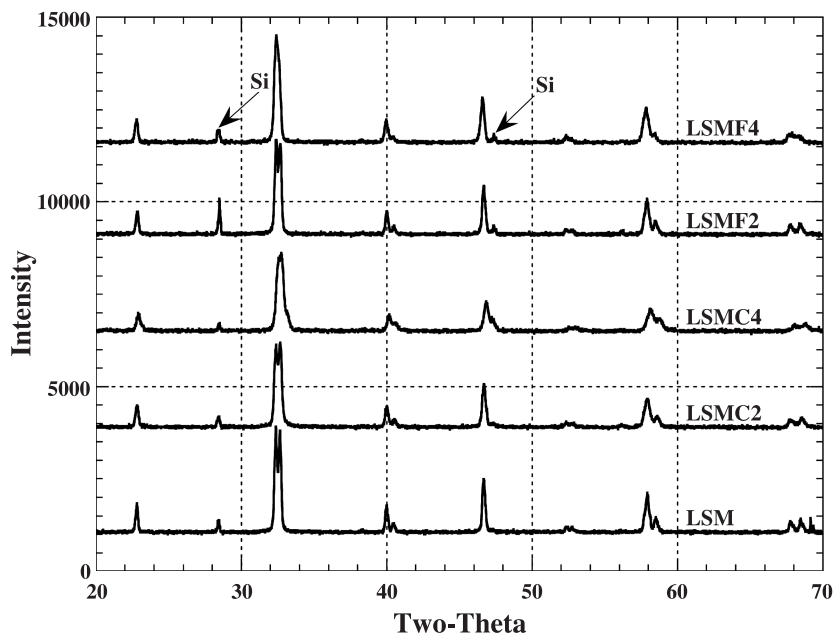


Fig. 4. XRD patterns of calcined powder for the compositions of LSM, LSMC2, LSMC4, LSMF2 and LSMF4.

Table 1
Lattice parameters and X-ray density of calcined powders

| Compositions | Symmetry | Calculated lattice parameters | | | | Cell volume ($\text{Å}^3$) | X-ray density ($\text{g cm}^{-3}$) |
|---|---|---|---|---|---|---|---|
| | | $a$ (Å) | $b$ (Å) | $c$ (Å) | $\beta$ | | |
| LSM | Monoclinic | 5.491 | 5.529 | 7.784 | 90.59 | 236.308 | 6.57 |
| LSMC2 | Monoclinic | 5.480 | 5.523 | 7.780 | 90.49 | 235.461 | 6.62 |
| LSMC4 | Monoclinic | 5.479 | 5.509 | 7.772 | 90.10 | 234.589 | 6.66 |
| LSMF2 | Monoclinic | 5.480 | 5.536 | 7.788 | 90.67 | 236.250 | 6.58 |
| LSMF4 | Orthorhombic | 5.535 | 5.529 | 7.796 | – | 238.581 | 6.52 |

## 2.2. Characterization

The phases of all sintered compositions were determined by XRD to investigate the other existing phases after firing at higher temperature. The dc four-point electrical conductivity of the sintered rectangular bars was measured as a function of temperature. Fired-on gold electrode was applied on the specimens before measurement. The data were collected at every 5 °C with an increasing temperature of 4 °C/min from 100 to 900 °C. The linear thermal expansion of sintered compositions was investigated by dilatometer (Netzsch, Dil402C). The microstructure of the specimens was observed by scanning electron microscope (Jeol, JSM5410). All specimens were polished and then thermally etched before gold sputtering.

## 3. Results and discussion

The XRD pattern of lanthanum oxide as-received raw material appeared in Fig. 1 shows the additional diffraction

peaks of $2\theta$ at 27.3, 28.0 and 47.8, indicating the other phase, possibly La(OH)$_3$. Only single phase of La$_2$O$_3$ can be observed after calcination at 1000 °C. In addition, the DTA and TGA results of received La$_2$O$_3$ illustrated in Fig. 2 represent the decomposition reactions around 350 °C and 500 °C, respectively. Both the endothermic reactions and the weight loss are possibly attributed to the water removal from La(OH)$_3$. As a consequence, La$_2$O$_3$ was calcined before weighing for sample preparation.

Fig. 3 exhibits the DTA results of mixed raw materials for the compositions of LSM, LSMC4 and LSMF4. The data indicate that the reaction peaks of LSMC4 and LSMF4 are similar to those of undoped LSM and the reactions complete before 1000 °C. However, the higher calcination temperature and holding at the reaction temperature are necessary to complete the reactions for a large amount of powder. In this work, calcining at 1200 °C is used for all compositions to obtain a uniform phase. The single phase of all calcined powder is identified by XRD and revealed in Fig. 4. The results indicate the monoclinic structure for LSM, LSMC2, LSMC4, LSMF2 and the orthorhombic structure for LSMF4 as observed on the only one peak of $2\theta$ at 32.5. The calculated lattice parameters and unit cell volumes of all calcined powder are also listed in Table 1. After firing at 1450 °C, the existing phases of all sintered pellets are shown in Fig. 5. Obviously, the appearance of extra peaks as indicated by the arrows can be seen in Co- and Fe-doped LSM, suggesting a separation of phases taking place after sintering at higher temperature. For LSMC2 and LSMC4, the alumina substrates appear to be blue around the sintered samples due to the chemical unstability of cobalt in the composition. For Fe-doped LSM, the amount of second phase increases with the Fe content as illustrated by the strongest peak of $2\theta$ at 20.8.
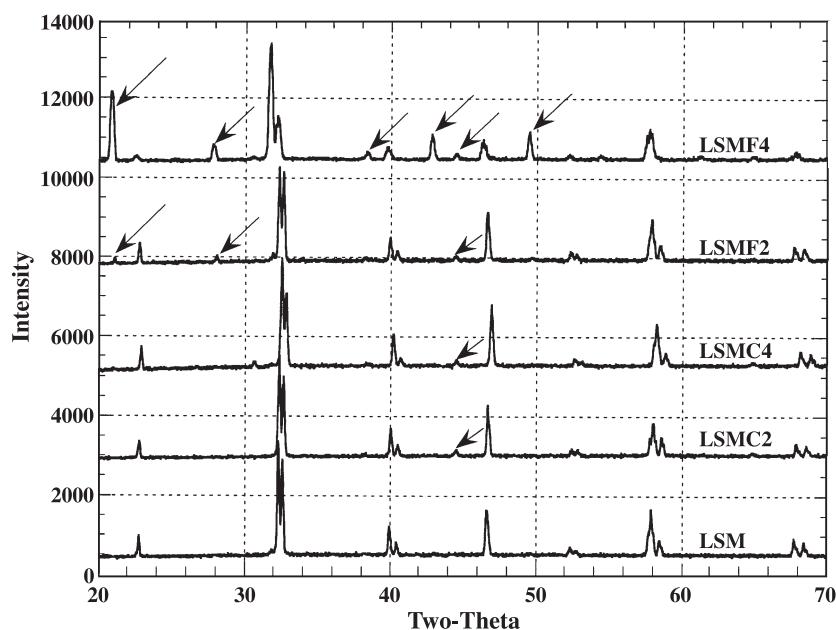


Fig. 5. XRD patterns of LSM, LSMC2, LSMC4, LSMF2 and LSMF4 sintered at 1450 °C.
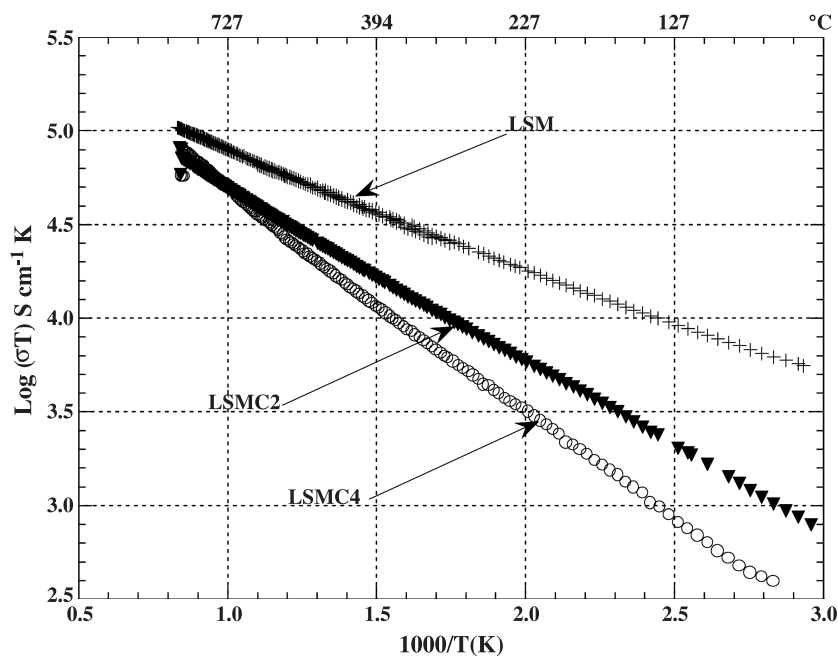
Fig. 6. Electrical conductivity vs. reciprocal temperature of LSM, LSMC2 and LSMC4.

The results of temperature dependence on the conductivity of Co- and Fe-doped LSM are illustrated in Figs. 6 and 7, respectively. There is no evidence of phase transitions in all sintered compositions because abrupt change of the slope in the conductivity plot is not observed. The electrical conductivity at 1000 °C and the activation energy of all compositions are calculated and summarized in Table 2. Undoped LSM shows the highest $\sigma_{1000\ °C}$ of 99.33 S/cm. This value is less than the reported by other researchers (133 S/cm [2] and 170 S/cm [3]). The reasons for different conductivity values are possibly due to the presence of second phase and the difference in preparation condition such as synthesis method and firing condition.

An addition of 20 mol% Co into LSM decreases its conductivity, as shown in Fig. 6. Nevertheless, with 40 mol% Co, the conductivity at high temperature tends to increase. These results can be explained by electron–hole charge compensation. The conductivity of lanthanum strontium manganite occurs by hole-hopping conduction, but for lanthanum strontium cobaltite, the conductivity is dominat-ed by electron [12]. Therefore, the electrons from 20 mol% Co might associate with holes obtained from lanthanum strontium manganite and the net charge carriers reduce, corresponding to decrease the conductivity as compared to LSM. With 40 mol% Co, the number of electrons increases and the conductivity shifts upward.

In contrast, the conductivity of Fe-doped LSM decreases with an increase of Fe content as revealed in Fig. 7. This is potentially attributed to a reduction of available sites for hole hopping conduction and the presence of other phases as illustrated in XRD results on Fig. 5. The higher Fe dopants increase the amount of second phase, therefore decreasing the conductivity of LSM.

Fig. 8a–d shows the SEM micrographs of all polished samples after sintering at 1450 °C. Both the intergranular and intragranular pores can be observed in all compositions. Co dopant (20 mol%) does not influence the grain size of LSM, but 40 mol% Co significantly reduces the grain size to about 5–10 μm. On the contrary, the average grain size increases as Fe content increases.

The values of TEC, from 100 to 900 °C of all compositions, are listed in Table 2. The TEC of LSM is $11.62 \times 10^{-6}\ K^{-1}$, which is slightly different from other reports ($11.9 \times 10^{-6}\ K^{-1}$ [3] and $12.63 \times 10^{-6}\ K^{-1}$ [4]). Its TEC depends on the amount of Co. In contrast, TEC slightly decreases as Fe content increases.

## 4. Conclusions

Both the 20 and 40 mol% Co-doped $La_{0.84}Sr_{0.16}MnO_3$ exhibit monoclinic structure like the undoped composition (LSM). The undoped LSM provides the highest conductiv-

Table 2
Calculated $\sigma_{1000\ °C}$, $E_a$ and thermal expansion coefficient of specimens sintered at 1450 °C

| Composition | $\sigma_{1000\ °C}$ (S cm$^{-1}$) | $E_a$ (kJ mol$^{-1}$) | TEC (100–900 °C) ($\times 10^{-6}$ K$^{-1}$) |
|---|---|---|---|
| LSM | 99.33 | 11.61 | 11.62 |
| LSMC2 | 61.55 | 17.98 | 11.69 |
| LSMC4 | 77.33 | 23.69 | 13.65 |
| LSMF2 | 59.20 | 17.38 | 11.58 |
| LSMF4 | 19.77 | 19.77 | 11.55 |
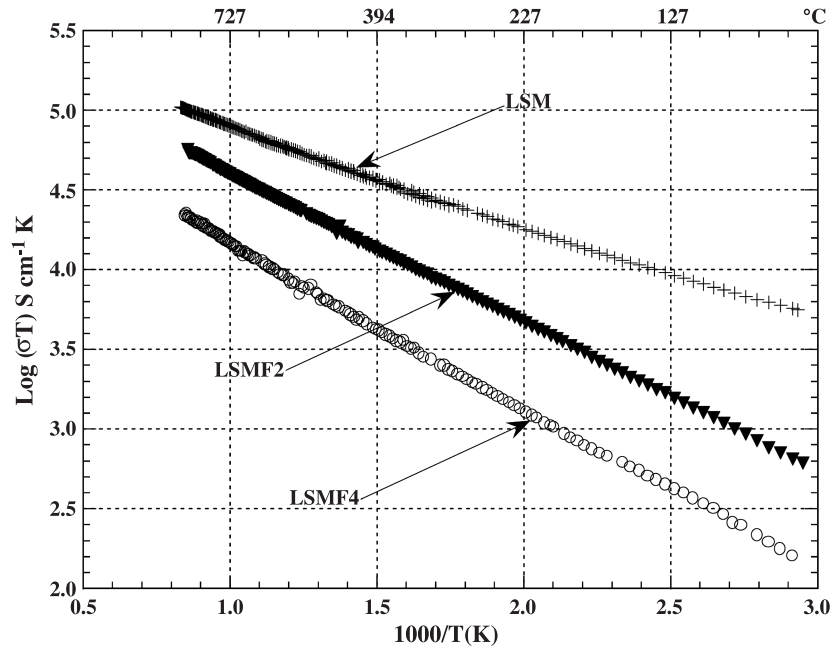
Fig. 7. Electrical conductivity vs. reciprocal temperature of LSM, LSMF2 and LSMF4.

ity at 1000 °C of 99.33 S/cm. Doped with 20 mol% Co, its electrical conductivity decreases. However, it tends to increase at high temperature as the amount of Co in LSM increases. In addition, Co inhibits the grain growth of undoped LSM. The thermal expansion coefficient of LSM increases with the amount of Co.
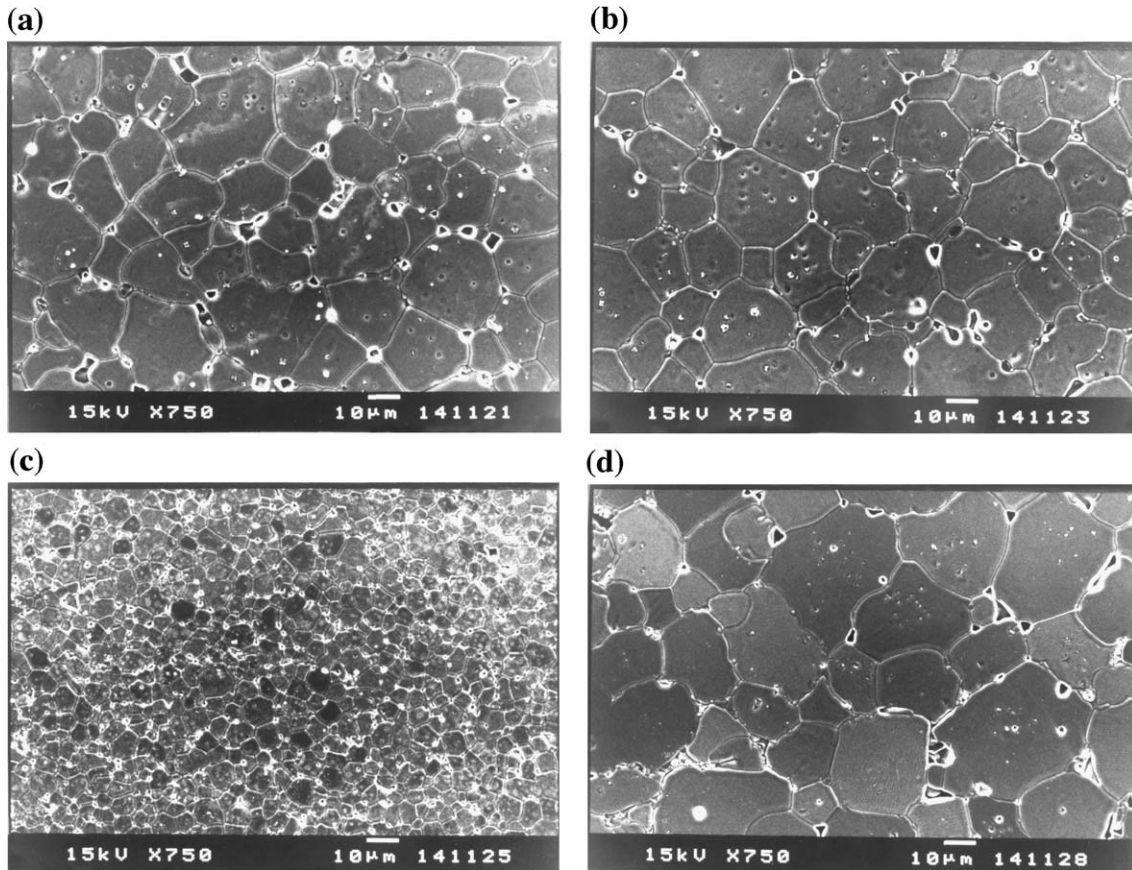


Fig. 8. SEM micrographs of the compositions sintered at 1450 °C. (a) LSM. (b) LSMC2. (c) LSMC4. (d) LSMF4.

In contrast, the structure of Fe-doped LSM changes from monoclinic to orthorhombic as the Fe content increases from 20 to 40 mol%. The electrical conductivity decreases with increasing amount of Fe due to the formation of second phase. In addition, the higher amount of Fe performs the larger grain size but insignificantly affects the thermal expansion coefficient.

## Acknowledgements

## References

[1] N.Q. Minh, T. Takahashi, Science and Technology of Ceramic Fuel Cells, Elsevier, The Netherlands, 1995.

[2] M. Kertesz, I. Riess, D.S. Tannhauser, R. Langpape, F.J. Rohr, J. Solid State Chem. 42 (1982) 125.

[3] A. Mackor, M. Koster, G. Kraaijkamp, J. Gerretsen, M. Van Eijk, Proceedings of the 2nd International Symposium on SOFCs, 1991, p. 463.

[4] T. Aruna, M. Muthuraman, C. Patil, J. Mater. Chem. 7 (1997) 2499.

[5] B. Gharbage, F. Mandier, H. Lauret, C. Roux, T. Pagnier, Solid State Ion. 82 (1995) 85.

[6] J.A. Labrincha, J.R. Frade, F.R.B. Marques, J. Mater. Sci. 28 (1993) 3809.

[7] G. Stochniol, E. Syskakis, A. Naoumidis, J. Am. Ceram. Soc. 78 (4) (1995) 929.

[8] K. Wiik, C.R. Schmidt, S. Faaland, S. Shamsili, M. Einarsrud, T. Grande, J. Am. Ceram. Soc. 82 (3) (1999) 721.

[9] L. Kindermann, D. Das, H. Nickel, K. Hilpert, J. Electrochem. Soc. 144 (1997) 717.

[10] L. Kindermann, D. Das, D. Bahadur, R. Weiss, H. Nickel, K. Hilpert, J. Am. Ceram. Soc. 80 (4) (1997) 909.

[11] D.L. Meixner, R.A. Cutler, Solid State Ion. 146 (2002) 273.

[12] R. Lankhorst, M. Bouwmeester, J. Electrochem. Soc. 144 (1997) 1261.